HHS Public Access

Author manuscript

Brain Behav Immun. Author manuscript; available in PMC 2019 March 01.

Published in final edited form as:

Brain Behav Immun. 2018 March ; 69: 568–581. doi:10.1016/j.bbi.2018.02.004.

Changes in motor function, cognition, and emotion-related behavior after right hemispheric intracerebral hemorrhage in various brain regions of mouse

Wei Zhu[a,b], **Yufeng Gao**[a], **Jieru Wan**[a], **Xi Lan**[a], **Xiaoning Han**[a], **Shanshan Zhu**[c], **Weidong Zang**[d], **Xuemei Chen**[d], **Wendy Ziai**[a,e], **Daniel F. Hanley**[e], **Scott J. Russo**[f], **Ricardo E. Jorge**[g], and **Jian Wang**[a,*]

[a]Department of Anesthesiology and Critical Care Medicine, Johns Hopkins University School of Medicine, Baltimore, Maryland 21205, USA

[b]Department of Emergency Medicine, Tongji Hospital, Tongji Medical College, Huazhong University of Science and Technology, Wuhan, Hubei 430030, PR China

[c]Department of Psychiatry and Behavioral Sciences, Johns Hopkins University, School of Medicine, Baltimore, Maryland 21205, USA

[d]Department of Human Anatomy, Basic Medical College of Zhengzhou University, Zhengzhou 450001, Henan, PR China

[e]Department of Neurology, Johns Hopkins University School of Medicine, Baltimore, Maryland 21205, USA

[f]Fishberg Department of Neuroscience and Graduate School of Biological Sciences, Icahn School of Medicine at Mount Sinai, New York, NY, USA

[g]Department of Psychiatry and Behavioral Sciences, Baylor College of Medicine, Houston, Texas, USA

Abstract

Intracerebral hemorrhage (ICH) is a detrimental type of stroke. Mouse models of ICH, induced by collagenase or blood infusion, commonly target striatum, but not other brain sites such as ventricular system, cortex, and hippocampus. Few studies have systemically investigated brain damage and neurobehavioral deficits that develop in animal models of ICH in these areas of the right hemisphere. Therefore, we evaluated the brain damage and neurobehavioral dysfunction associated with right hemispheric ICH in ventricle, cortex, hippocampus, and striatum. The ICH model was induced by autologous whole blood or collagenase VII-S (0.075 units in 0.5 μl saline)

*Correspondence to: Jian Wang, MD, PhD, Department of Anesthesiology and Critical Care Medicine, Johns Hopkins University School of Medicine, 720 Rutland Ave, Ross Bldg 370B, Baltimore, MD 21205 (Phone: 443.287.5490; jwang79@jhmi.edu).

Conflict of interest

The authors declare that they have no conflict of interest.

injection. At different time points after ICH induction, mice were assessed for brain tissue damage and neurobehavioral deficits. Sham control mice were used for comparison. We found that ICH location influenced features of brain damage, microglia/macrophage activation, and behavioral deficits. Furthermore, the 24-point neurologic deficit scoring system was most sensitive for evaluating locomotor abnormalities in all four models, especially on days 1, 3, and 7 post-ICH. The wire-hanging test was useful for evaluating locomotor abnormalities in models of striatal, intraventricular, and cortical ICH. The cylinder test identified locomotor abnormalities only in the striatal ICH model. The novel object recognition test was effective for evaluating recognition memory dysfunction in all models except for striatal ICH. The tail suspension test, forced swim test, and sucrose preference test were effective for evaluating emotional abnormality in all four models but did not correlate with severity of brain damage. These results will help to inform future preclinical studies of ICH outcomes.

Keywords

cognition; emotion; intracerebral hemorrhage; motor

1. Introduction

Factors that predict short-term mortality after intracerebral hemorrhage (ICH) are fairly well known, but little is understood about long-term functional outcomes (Moulin and Cordonnier, 2015). Patients with ICH experience not only locomotor and memory impairment (Brainin et al., 2015; Langhorne et al., 2009) but frequently depression as well (Christensen et al., 2009; Hacket and Pickles, 2014; Koivunen et al., 2015). For example, ICH in the frontal cortex can lead to cognitive dysfunction and emotional changes (Lee et al., 2012; Moulin et al., 2016; Tang et al., 2011). Additionally, intraventricular hemorrhage (IVH), which occurs as an extension of intraparenchymal hemorrhage or subarachnoid hemorrhage into the ventricular system (Hallevi et al., 2008; Hwang et al., 2012), is associated with increased cognitive deficits and mortality (Brand et al., 2014; Hinson et al., 2010). Although the hippocampus is not a common site of bleeding, damage to it can cause deficits in memory and social interaction (Rubin et al., 2014).

Most animal models that have been developed to mimic the clinical progression of ICH target the striatum (Keep et al., 2012; MacLellan et al., 2011; Wang, 2010; Wang and Dore, 2007). Few studies have modeled ICH in the ventricular system, cortex, and hippocampus, despite their clinical prevalence. Moreover, the behavioral tests used in rodent models of ICH focus primarily on functional deficits and recovery after striatal ICH in the left hemisphere. Very few studies have evaluated the cognitive and emotional changes associated with ICH in the right hemisphere.

Many tests exist to assess locomotor function, grip and forelimb strength, memory, and emotion-related behavior in rodents subjected to ICH models. These include the 24-point neurologic deficit score (Han et al., 2016; Wang et al., 2003), wire-hanging test and cylinder test (Auriat and Colbourne, 2009; Lan et al., 2017a; Manaenko et al., 2009), novel object recognition test (Perez-Urrutia et al., 2017; Yang et al., 2017b), tail suspension test, forced

swim test, and sucrose preference test (Perez-Urrutia et al., 2017; Zhu et al., 2017). However, these tests have been used primarily to evaluate cognitive and emotion-related behavioral changes after striatal ICH and rarely applied to ICH models of the right lateral ventricle, cortex, and hippocampus. Therefore, our goal was to characterize brain damage and functional outcomes in ICH models that affect right-hemispheric structures using histology, immunofluorescence, and a battery of behavioral tests to evaluate motor, cognitive, and emotion-related behavior. We hypothesized that brain damage and behavioral deficits after ICH differ by brain region affected.

2. Materials and methods

2.1 Mice

This study was conducted in strict accordance with the recommendations in the *Guide for the Care and Use of Laboratory Animals* published by the National Institutes of Health. Animal use protocols were approved by the Johns Hopkins University Animal Care and Use Committee (Approved protocol number: MO15M83). Measures were taken to minimize the number of laboratory mice used and to ensure minimal pain and discomfort. Adult male C57BL/6 mice (20–25 g, total n=433) were placed into a clean induction chamber and anesthetized by isoflurane (3–4% initially and 1–2% for maintenance, Baxter healthcare Co.) in an oxygen-air mixture (20%:80%). Rectal temperature was monitored with a thermometer and maintained at 37 ± 0.5°C by an electronic thermostat-controlled warming blanket (Stoelting Co.) throughout the surgical procedure.

2.2 Experimental groups and surgical procedures

2.2.1 Striatal intracerebral hemorrhage (s-ICH)—Mice were placed in a stereotaxic frame (RWD Life Science) and infused in the right striatum with either 10 μl (low-dose group, n=12) or 30 μl (high-dose group, n=10) of autologous whole blood. Based on a published protocol with minor modifications (Krafft et al., 2012; Rynkowski et al., 2008; Wang et al., 2008a), we made a midline scalp incision and drilled a hole into the right side of the skull (for infusion of 10 μl blood: 0.6 mm anterior and 2.0 mm lateral of the bregma; for infusion of 30 μl blood: 0.2 mm anterior and 2.0 mm lateral of the bregma). The mouse's tail was immersed in warm water (40 °C) for 2 min, and the tail skin cleaned with 70% alcohol. Blood was quickly drawn from the central tail artery with a sterile needle (25-gauge) (Zhu et al., 2014) into a sterile 50-μl Hamilton syringe without anticoagulant. After blood collection, the Hamilton syringe was secured onto a motorized micro-injector (Stoelting Co.), and the blood was infused at a rate of 1 μl/min. For the low-dose group, 4 μl of blood was infused at 3.0 mm below the surface of the skull, and then after a 5-min pause, the remaining 6 μl of blood was infused at a depth of 3.8 mm. The needle was withdrawn at a rate of 1 mm/min beginning 10 min after the second injection. For the high-dose group, mice were similarly infused with 5 μl and 25 μl of blood. The burr hole was filled with bone wax (Ethicon, Somerville, NJ), and the scalp incision was closed with Super Glue (Henkel Consumer Adhesive Inc. Scottsdale, Arizona). Mice in the sham group (n=8) received only needle insertion into the right striatum.

2.2.2 Intraventricular hemorrhage (IVH)—Either 25 μl (low-dose group, n=12) or 40 μl (high-dose group, n=10) of autologous whole blood was infused into the right lateral brain ventricle. A 26-gauge needle attached to a Hamilton syringe was stereotaxically inserted into the right ventricle 2.5 mm below the surface of the skull (coordinates: 0.5 mm posterior and 1.0 mm lateral of the bregma) and autologous blood was infused at a rate of 5 μl/min. After the infusion, the needle was left in place for 10 min and then removed at a rate of 1 mm/min. Mice in the sham group (n=8) were injected with an equal amount of saline.

2.2.3 Cortical intracerebral hemorrhage (c-ICH)—The c-ICH model was produced according to previous studies (Masuda et al., 2010; Zhu et al., 2014) with minor modifications. Each mouse (n=10) was stereotaxically injected with collagenase (Type VII-S, 150 U/ml, sterile-filtered, high purity, purified by chromatography, Sigma-Aldrich Co.) at two sites of the right cortex at the following stereotactic coordinates: site 1: 0.0 mm anterior and 1.5 mm lateral of the bregma, 1.6 mm in depth; site 2: 1.0 mm anterior and 2.0 mm lateral of the bregma, 1.6 mm in depth. The low-dose group received 0.3 μl per site, and the high-dose group received 0.4 μl per site at a rate of 0.1 μl/min. The needle was withdrawn slowly 20 min after each injection to minimize backflow. Mice in the sham group (n=8) received an injection of the same amount of saline into each site. We chose these volumes because larger volumes did not produce well-defined hematomas.

2.2.4 Hippocampal intracerebral hemorrhage (h-ICH)—Mice (n=10) were injected with 0.2 μl of collagenase at a rate of 0.1 μl/min in the right hippocampus at 2.5 mm posterior and 1.7 mm lateral of the bregma, 1.8 mm in depth (Rogove et al., 2002). The needle was withdrawn slowly 10 min after injection. Mice in the sham group (n=8) were injected with 0.2 μl of saline. We chose this volume because in preliminary experiments, 0.3 μl and 0.1 μl of collagenase failed to produce a well-defined hematoma.

2.3 Behavioral tests

Mice were housed in a temperature- and humidity-controlled room that was maintained on a 12-h light/dark cycle, with food available ad libitum. All behavioral tests were conducted during the light cycle phase in enclosed behavior rooms. The same mice were used for all behavioral tests (Supplementary Fig. 1). All behavioral tests were evaluated and analyzed by an observer blinded to the study. Data were mapped with Graphpad Prism 5 software (GraphPad Software, Inc. USA).

2.3.1 Assessment of neurologic deficits—Neurologic function of each mouse was tested on days 1, 3, 7, 14, and 21 post-ICH with assessments of body symmetry, gait, climbing, circling behavior, front limb symmetry, and compulsory circling (Wu et al., 2017). Each test was graded from 0 to 4, establishing a maximum deficit score of 24.

2.3.2 Wire-hanging test—We evaluated grip strength, balance, and endurance in each mouse with the wire-hanging test on days 1, 3, 7, 14, and 21 post-ICH. Mice used their forelimbs to suspend their body weight on a 55 cm long iron wire stretched between two posts 50 cm above the ground. The hind limbs were gently covered with adhesive tape to

prevent them from using all four paws. A pillow was used to prevent fall injuries (Zhu et al., 2014). The time that each mouse remained on the wire was recorded.

2.3.3 Cylinder test—We used the cylinder test to assess forelimb preference and asymmetry in each mouse on days 1, 3, 7, 14, and 21 post-ICH. According to a previously published method (Vahid-Ansari et al., 2016), we placed the mouse in a transparent cylinder (height 16.5 cm, diameter 9 cm) with two mirrors arranged at an angle behind the cylinder. A camera recorded forelimb usage during rearing and exploratory behavior for 5 min. We analyzed the videos to determine how many times each forelimb made wall contact. We used the following criteria: (1) The first forelimb to contact the wall during a full rear was considered an independent wall placement and recorded as a “left” or “right.” (2) Simultaneous contact by the left and right forelimb during a full rear and for lateral movements along the wall was recorded as “both.” (3) If the two forelimbs contacted the wall in quick succession without removal of the first, we recorded the movement as “left or right (the first contacted) forelimb independent” and “both.” (4) When the mouse explored the wall laterally, alternating both forelimbs, it was recorded as a “both” movement. The final score was calculated as: (Right forelimb movement − Left forelimb movement)/(Right forelimb movement + Left forelimb movement + both movement).

2.3.4 Novel object recognition test—The novel object recognition test was performed on day 21 post-ICH as described previously (Yang et al., 2017b; Zhu et al., 2014). In brief, mice were habituated to an open field (47×26×20 cm) for 5 min on day 1. On day 2 they were exposed to two identical novel objects (green cubes, 4×4×3cm) for 10 min. After 1 h, they were exposed to one novel object (white ball, 5 cm in diameter) and one familiar object (green cube) for 5 min. All behavior was recorded on video. A discrimination index (total time spent with new object/total time devoted to exploring objects) was calculated for each experimental group. Exploration of the object was defined as any direct contact with mouth, nose, or paw, or the nose directed at the object at <0.5 cm. Contacts judged to be accidental and standing, sitting, or leaning on the object were excluded (Besheer and Bevins, 2003).

2.3.5 Tail suspension test—Each mouse was subjected to the tail suspension test on days 7, 14, and 21 according to an established protocol (Can et al., 2012b; Zhu et al., 2014). Mice were acclimated to the behavior room for 1 h and then suspended by their tails to the edge of a shelf 55 cm above the floor. Adhesive tape (17 cm long) attached the tail (approximately 1 cm from the tip of the tail) to the shelf. A plastic tube (4 cm long, 1 cm diameter, 1.5 g) placed around the tails blocked their ability to climb them. A camera recorded their movements for 6 min, and we determined the duration of mobility. The total duration of mobility was subtracted from the 360 seconds of test time and recorded as the immobility time. Mice were considered immobile only when they hung passively and completely motionless.

2.3.6 Forced swim test—We tested mice with the forced swim test (Can et al., 2012a; Zhu et al., 2014) on day 22 after ICH to prevent influence from the stress of the tail suspension test on day 21. Mice were acclimated to the behavior room 1 h before being placed individually in 20 cm high cylindrical tanks (22 cm in diameter) containing 10 cm of

water at 24 ± 1 °C. The movements of the mice were recorded by a camera for 6 min, and we determined the duration of mobility during the last 4 min. The total mobility time was subtracted from the 240 seconds of test time and recorded as the immobility time. Mice that were floating upright and making only small movements to remain above water were considered to be immobile (Renard et al., 2004).

2.3.7 Sucrose preference test—The sucrose preference test is used to assess anhedonia. On day 18, each mouse was placed in a separate cage with two tubes, one containing water and the other a 1% sucrose solution. The tubes were weighed at the beginning of the experiment, and their position in the cage was switched every day. On day 21, we re-weighed the two tubes and calculated the amount of liquid consumed from each. The sucrose preference was calculated as a percentage of the consumed sucrose solution relative to the total amount of liquid drunk: sucrose preference = sucrose consumption (g)/(water consumption (g) + sucrose consumption (g)). Anhedonia is characterized by a reduction in sucrose intake (De Bundel et al., 2013; Zhe et al., 2017).

2.4 Histologic morphology

Mice were sacrificed on days 3 (n = 6/group) and 22 post-ICH (n = 5/group). The entire brain of each mouse was cut into 50-μm-thick sections with a cryostat. All sections from the s-ICH, c-ICH, and h-ICH groups that contained hematoma were selected and stained with Luxol fast blue (for myelin) and Cresyl violet (for neurons). Sections from the IVH group that contained hematoma were stained with Cresyl violet only. SigmaScan Pro software (version 5.0.0 for Windows; Systat, San Jose, CA) was used to quantify the gray and white matter injury and volume of ventricles on day 3 post-ICH and to quantify the volume of whole brain, cortex, ventricle, and hippocampus on day 22 post-ICH (Jacobs et al., 1990; Masuda et al., 2010; Sherry et al., 1993). The injury volume and volume of whole brain, cortex, ventricle, and hippocampus in cubic millimeters was calculated by multiplying the thickness by the sum of the damaged areas of each section (Li et al., 2017a; Wang et al., 2003). Sections were analyzed by an investigator blinded to the experimental cohort.

2.5 Histology

Mice in each group were anesthetized and perfused via cardiac catheter with 4% paraformaldehyde in 0.1 mol/l phosphate-buffered saline (pH 7.4) on day 3 after ICH. The brains were removed, placed in 4% paraformaldehyde for 24 h, and then immersed in 30% sucrose for 72 h at 4°C. The brains were then cut into 25-μm-thick coronal sections with a cryostat. Fluoro-Jade B (FJB) was used to quantify neuronal death (Li et al., 2017a). We selected three sections per mouse with similar areas of striatal, cortical, ventricular, or hippocampal hematoma to quantify FJB-positive cells. The numbers of FJB-positive cells from 12 randomly selected locations per mouse (4 fields per section × 3 sections per mouse) in the periventricular brain region (IVH model) or in the brain regions surrounding the hematoma (s-ICH, c-ICH and h-ICH models) were averaged and expressed as positive cells per square millimeter (n = 6/group). Sections were analyzed by an investigator blinded to the experimental cohort.

2.6 Brain water content

Brain edema was determined by the wet–dry weight ratio method as described previously (Yang et al., 2017a; Zhu et al., 2014). Briefly, mice (n = 4–5/group) were sacrificed by decapitation 72 h post-ICH. The brains were removed immediately and cut from 4 to 7 mm posterior to the bregma in the s-ICH group, from 1 mm anterior to the bregma to 3 mm posterior to the bregma in the IVH group, from 3 mm anterior to the bregma to 2 mm posterior to the bregma in the c-ICH group, or from 0.8 mm to 4 mm posterior to the bregma in the h-ICH group. In the s-ICH, IVH, and c-ICH groups, the brains were dissected into five parts: ipsilateral and contralateral basal ganglia, ipsilateral and contralateral cortex, and cerebellum (which served as an internal control). In the h-ICH group, the brains were dissected into ipsilateral and contralateral hippocampus, ipsilateral and contralateral cortex, and cerebellum. Brain samples were weighed immediately on an analytical balance (Denver Instrument Co.) to obtain the wet weight and then dried at 100°C for 48 h to obtain the dry weight. Brain edema was expressed as (wet weight–dry weight)/wet weight of brain tissue × 100%.

2.7 Immunofluorescence

Sections (n = 6) were incubated with rabbit anti-Iba 1 primary antibody (microglial marker; 1:500; Wako Chemicals, Richmond, VA) followed by Alexa 488-conjugated goat anti-rabbit secondary antibody (1:1000; Molecular Probes, Eugene, OR). An investigator blinded to experimental cohort examined the stained sections under a fluorescence microscope (Eclipse TE2000-E, Nikon, Tokyo, Japan) and counted the immunoreactive cells over a 40× microscopic field from 12 randomly selected locations per mouse (4 fields per section × 3 sections per mouse) in the periventricular brain region (IVH model) or in the perihematomal brain regions (s-ICH, c-ICH, and h-ICH models). Numbers were averaged and expressed as positive cells per square millimeter.

2.8 Statistical analysis

All data are expressed as mean ± SD. Histology data were analyzed by one-way ANOVA followed by a post hoc analysis with Newman–Keuls method to correct for multiple comparisons. Behavioral tests were analyzed by two-way ANOVA and a post hoc analysis with Kruskal–Wallis for different time points, and one-way ANOVA with a post hoc analysis with Dunnett's method. Group differences were considered statistically significant at $P < 0.05$. Power calculations were performed with G*Power 3.1 software (Faul et al., 2007). Linear regression was used for correlational analysis, and a P-value < 0.05 was considered statistically significant.

3. Results

The mortality of mice was 6 of 84 (7.1%) in the s-ICH group, 7 of 85 (8.2%) in the IVH group, 4 of 80 (5.0%) in the c-ICH group, and 4 of 41 (9.8%) in the h-ICH group. No animals died in any of the sham groups (0 of 143).

3.1 Hemorrhagic injury volume and ventricular volume 72 h post-ICH

Volume of affected tissue and hemispheric enlargement were significantly greater in the s-ICH groups (10 μl and 30 μl) than in the respective sham groups. Additionally, the volume of affected tissue and degree of hemispheric enlargement were greater in the group injected with 30 μl of autologous blood than in the group injected with 10 μl of autologous blood (Fig. 1A). At 72 h after collagenase injection, hematoma was present in the cortex of the c-ICH groups (Fig. 1B) and in the hippocampus of the h-ICH group (Fig. 1C). Quantification showed significantly larger injury volume and hemispheric enlargement in the c-ICH group (Fig. 1B) and h-ICH group (Fig. 1C) than in their respective sham controls. Additionally, in the c-ICH model, the degree of injury volume and hemispheric enlargement was greater in the high-dose group than in the low-dose group ($P < 0.01$; Fig. 1B). In the IVH groups (25 μl and 40 μl), Cresyl violet staining revealed enlargement of the ventricles at 72 h after blood infusion, but the difference between the high-dose (40 μl) and low-dose (25 μl) IVH groups was not statistically significant ($P > 0.05$; Fig. 1D).

3.2 Volume of whole brain, cortex, and hippocampus on day 22 post-ICH

The volume of striatum in both s-ICH groups (10 μl and 30 μl) was smaller than that in the sham groups ($P < 0.01$). The volume of right cortex in the s-ICH groups (10 μl and 30 μl) was smaller than that in the respective sham groups ($P < 0.01$), whereas the volume of hippocampus showed little change from that in the sham groups (n=5 mice/group, $P > 0.05$; Supplementary Fig. 2A).

The cortical and hippocampal volumes in both hemispheres of the IVH groups (25 μl and 40 μl) were smaller than those of the respective sham groups, whereas the ventricular volume was greater than that in the sham groups. The volume of whole brain was less in the high-dose (40 μl) and low-dose (25 μl) IVH groups than that in the sham group (n=5 mice/group, $P < 0.01$–0.05; Supplementary Fig. 2B).

In the c-ICH groups, the cortical and hippocampal volumes in ipsilateral hemisphere were smaller than those in the respective sham groups. However, volumes on the contralateral side were unchanged from those in the sham groups. Further, the volume of whole brain was smaller in the c-ICH groups than in the sham group. In the h-ICH group, cortical volume and hippocampal volume in the ipsilateral hemisphere were smaller than those in the sham groups (n=5 mice/group, $P < 0.01$; Supplementary Fig. 2C and 2D).

3.3 Neuronal death

FJB staining was used to detect neuronal degeneration at 72 h post-ICH (Cheng et al., 2016). Compared with sham groups, the s-ICH, c-ICH, and h-ICH mice exhibited more FJB-positive cells around the injury sites in the striatum, cortex, and hippocampus, respectively (Fig. 2A, B, D). Similarly, IVH mice exhibited greater numbers of FJB-positive cells around the lateral ventricles than did the sham controls (Fig. 2C). Quantification analysis confirmed also that brains of mice in the high-dose groups had significantly more FJB-positive cells than brains of mice in the respective low-dose groups. Furthermore, we observed more FJB-positive cells in the hippocampus of ICH mice than in the hippocampus of sham mice in all groups except for the s-ICH group (n=6 mice/group, $P < 0.01$; Fig. 3A–D).

3.4 Brain water content

Brain water content was elevated compared with that in sham groups at 72 h post-ICH in the ipsilateral basal ganglia of the s-ICH groups (10 μl and 30 μl; n=5 mice/group, $P < 0.05$–0.1; Fig. 4A), in the ipsilateral basal ganglia and cortex of the IVH groups (25 μl and 40 μl; n=5 mice/group, $P < 0.05$–0.1; Fig. 4B), in the ipsilateral cortex of the c-ICH group (n=5 mice/group, $P < 0.01$; Fig. 4C), and in the ipsilateral hippocampus of the h-ICH group (n=4 mice/group, $P < 0.01$; Fig. 4D). No differences in brain water content were observed between the low- and high-dose groups within the s-ICH, IVH, and c-ICH models ($P > 0.05$; Fig. 4A–C).

3.5 Neuroinflammation

We assessed microglia/macrophage activation because early cellular inflammation is known to contribute to secondary brain injury after ICH (Wang, 2010; Wang and Dore, 2007). We defined microglial/macrophage activation by morphologic criteria and a cell body diameter cutoff of 7.5 μm (Wu et al., 2010). At 72 h after ICH, activated microglia/macrophages were evident in the brain regions around the lateral ventricles in mice exposed to IVH and around the injury sites in the striatum, cortex, and hippocampus of mice exposed to the s-ICH, c-ICH, and h-ICH models, respectively (Fig. 5A–D). Quantification analysis confirmed that mice subjected to ICH had significantly more activated microglia/macrophages than did sham mice. Moreover, significantly more Iba1-positive activated microglia/macrophages were present in the brains of mice in the high-dose s-ICH and c-ICH groups than in those of mice in the low-dose s-ICH and c-ICH groups, respectively (n=6 mice/group, $P < 0.01$). The number of activated microglia/macrophages correlated positively with the volume of the affected brain tissue of mice on day 3 in both the 10- μl and 30-μl s-ICH groups (r=0.89, 0.84, respectively; both $P < 0.05$; Supplementary Fig. 3A and 3B).

3.6 Locomotor function

Based on results from the 24-point neurologic scoring system, wire-hanging test, and cylinder test, we found that s-ICH mice (10 μl and 30 μl) demonstrated marked deficits in locomotor activity, gripping, and forelimb strength compared with those of sham mice at all time points tested (power=0.99 in both the 24-point neurologic scoring system and wire-hanging test). Additionally, the neurologic deficit scores were significantly higher in high-dose than in low-dose s-ICH mice on days 1, 3, and 7 post-ICH (n=10–12 mice/group, $P < 0.01$; Fig. 6A). In the cylinder test, scores were higher in s-ICH (10 μl and 30 μl) mice than in sham mice on days 1 and 3 post-ICH, but we observed no difference between high-dose and low-dose s-ICH mice. The mice exhibited complete recovery on day 7 post-ICH (n=10–12 mice/group, $P < 0.01$–0.05; power=0.63; Fig. 6A). Neurologic deficit score, but not performance in the wire-hanging test or cylinder test, correlated positively with the volume of affected brain tissue of mice on day 3 in the 10-μl and 30-μl s-ICH groups (r = 0.82, 0.88, respectively; both $P < 0.05$; Supplementary Fig. 4A and 4B). Neurologic deficit score also correlated positively with the number of activated microglia/macrophages in the perihematomal region of mice on day 3 in the two s-ICH groups (r = 0.67, 0.84, respectively; $P < 0.05$; Supplementary Fig. 5A and 5B)

Mice in the IVH (25 μl and 40 μl) groups had significantly higher neurologic deficit scores than did sham animals on days 1, 3, and 7 post-ICH, but we observed no significant

difference in deficit scores between the low- and high-dose IVH groups at any time point (n=10–12 mice/group, $P < 0.01$; power=0.99; Fig. 6B). In the wire-hanging test, IVH (25 μl and 40 μl) mice exhibited marked deficits in gripping and forelimb strength compared with those of sham animals on days 1, 3, and 7 post-ICH (n=10–12 mice/group, $P < 0.01$–0.05; power=0.92; Fig. 6B). However, scores in the cylinder test were unchanged from those in the sham group (n=10–12 mice/group, $P > 0.05$; power=0.13; Fig. 6B).

Mice in the c-ICH group had significantly higher neurologic deficit scores than did sham animals on days 1, 3, and 7 post-ICH (n=10 mice/group, $P < 0.01$; power=0.99; Fig. 6C). Locomotor deficit peaked on day 3, gradually recovered from day 7 to day 14, and returned to baseline on day 21. In the wire-hanging test, c-ICH mice exhibited marked deficits in gripping and forelimb strength compared with those of sham animals on days 1, 3, and 7 post-ICH (n=10 mice/group, $P < 0.01$; power=0.99; Fig. 6C). Mice had completely recovered from these deficits on days 14 and 21 post-ICH. Scores in the cylinder test were similar for c-ICH and sham mice (n=10 mice/group, $P > 0.05$; power=0.99; Fig. 6C).

Mice in the h-ICH group had significantly higher neurologic deficit scores than did sham animals on days 1, 3, and 7 post-ICH (n=10 mice/group, $P < 0.01$–0.05; power=0.88; Fig. 6D), but they recovered from days 7 to 21. In the wire-hanging test and cylinder test, we observed no difference between h-ICH mice and sham animals at any time point (n=10 mice/group, all $P > 0.05$; power=0.17, 0.55, respectively; Fig. 6D).

3.7 Memory function

In the novel object recognition test, we observed no differences between s-ICH (10 μl and 30 μl) mice and sham animals (n=10–12 mice/group, all $P > 0.05$; Fig. 7A). The discrimination index was significantly smaller in the IVH (25 μl and 40 μl), c-ICH, and h-ICH groups than in their respective sham groups. No difference was observed between low-dose and high-dose IVH mice (n=10–12 mice/group, $P < 0.01$–0.05; Fig. 7B–7D).

3.8 Changes in emotional state

Mice in the s-ICH groups (10 μl and 30 μl) exhibited significantly longer immobility time than sham animals in both the tail suspension test and forced swim test, but we observed no significant difference between the low- and high-dose s-ICH groups (n=10–12 mice/group, $P < 0.01$; Fig. 8A, B). Mice in the s-ICH groups (10 μl and 30 μl) also exhibited less sucrose preference than sham animals (n=10–12 mice/group, $P < 0.01$; Fig. 8A). Again, no difference was observed between the low- and high-dose groups.

Mice in the IVH groups (25 μl and 40 μl) had significantly longer immobility time in the tail suspension test than did sham animals on days 14 and 21 post-ICH (n=10–12 mice/group, $P < 0.01$; Fig. 8B). However, no significant difference was observed between the low-dose and high-dose IVH groups. In the forced swim test on day 22 post-ICH, mice in the IVH groups (25 μl and 40 μl) also exhibited significantly longer immobility time than did sham animals (n=10–12 mice/group, $P < 0.01$; Fig. 8B). Additionally, mice in the high-dose IVH group demonstrated less sucrose preference than the sham animals (n=10–12 mice/group, $P < 0.01$; Fig. 8B).

Mice in the c-ICH and h-ICH groups had significantly longer immobility times than their sham controls in the tail suspension test on days 14 and 21 post-ICH (n=10 mice/group, $P < 0.01$; Fig. 8C) and in the forced swim test on day 22. In the sucrose preference test, mice in the c-ICH and h-ICH groups exhibited significantly less sucrose preference than did sham animals (n=10 mice/group, $P < 0.01$; Fig. 8D).

We categorized animals as having depression-like behaviors if they scored at or above the median immobility time in the tail suspension test and forced swim test and at or below the median for sucrose preference. Depression-like behaviors developed in 5 of 12 mice (41.7%) in the low-dose (10 μl) s-ICH group, 4 of 10 mice (40%) in the high-dose (30 μl) s-ICH group, 5 of 12 mice (41.7%) in the low-dose (25 μl) IVH group, 5 of 10 mice (50%) in the high-dose (40 μl) IVH group, 5 of 10 mice (50%) in the low-dose (0.3 μl) c-ICH group, 5 of 10 mice (50%) in the high-dose (0.4 μl) c-ICH group, and 5 of 10 (50%) mice in the h-ICH group.

4. Discussion

In this study, we successfully established right hemispheric s-ICH, IVH, c-ICH, and h-ICH models in mice. Using histology, immunohistochemistry, and neurobehavioral tests, we validated that each model generated reproducible brain damage, brain edema, neuronal death, and neuroinflammatory responses. Furthermore, a series of behavior tests was applied to evaluate the locomotor function, cognitive function, and emotion-related behavioral deficits in these four ICH models. The behavioral tests revealed that ICH in different brain regions produces different behavioral deficits. We found that the 24-point neurologic scoring system was a sensitive method with the highest power to evaluate motor deficits in all four ICH models in the first week, whereas the novel object recognition test was capable of discriminating recognition memory dysfunction at the late stage in all models except for s-ICH. The tail suspension test, forced swim test, and sucrose preference test were effective for evaluating emotion-related behavior. Notably, we found that depression-like behavior was present in 40% to 50% of ICH mice based on the location of bleeding, a slightly higher percentage than that reported in clinical studies (Christensen et al., 2009; Koivunen et al., 2015; Wei et al., 2016).

Collagenase-induced ICH in rats has been reported to result in marked brain atrophy and long-term neurologic deficits at 10 weeks or 2 months post-ICH (Beray-Berthat et al., 2010; Hartman et al., 2009). In our study, the volume of cortex and striatum in ipsilateral hemisphere decreased in the s-ICH group, whereas the volume of hippocampus was unchanged on day 22 post-ICH. These results may indicate continued tissue loss after ICH. Neuronal death and brain water content were increased in the respective brain regions affected in the four ICH models at 72 h post-ICH.

We used a series of behavioral tests to evaluate neurologic function in our ICH models, but focused mostly on locomotor function. The 24-point neurologic deficit score is a very precise method of evaluating the overall locomotor function as demonstrated in previous studies (Jiang et al., 2016; Li et al., 2017a; Wu et al., 2010; Yang et al., 2017a). The wire-hanging test is a simple test to evaluate grip strength, balance, and endurance, and falling

latency was shown to be reduced in an s-ICH model (Manaenko et al., 2011). The cylinder test is used to assess forelimb use and rotation asymmetry, and animals exposed to s-ICH have demonstrated abnormal performance in this test (Wells et al., 2005). The results of our study were consistent with those of previous reports for s-ICH. s-ICH mice exhibited locomotor deficits in each of the tests. Moreover, mice in the high-dose s-ICH (30 μl) group had more severe neurologic deficits than mice in the low-dose s-ICH (10 μl) group on days 1, 3, and 7. These results indicate that the 24-point neurologic deficit score is sensitive enough to evaluate injury severity in the s-ICH model during the first week and are consistent with the results shown by MacLellan et al. (MacLellan et al., 2006). In that study, neurologic deficit scale, but not cylinder test, was able to distinguish among gradations in injury in the first week after ICH; the cylinder test was considered only as a “lesion detector.” We also obtained reproducible results from the wire-hanging test in mice that received pretraining. However, a positive correlation was detected only between neurologic deficit score and the number of activated microglia/macrophages in the perihematomal region or the volume of the affected brain tissue. The power analysis with G*Power 3.1 software for changes in locomotor function further indicated that the 24-point neurologic deficit scoring system was the most sensitive behavioral test for determining injury severity in the four ICH models. Nonetheless, selection of behavioral tests in preclinical efficacy studies should consider sensitivity to injury severity as well as the effects of treatments (MacLellan et al., 2006).

In our study, s-ICH mice exhibited both locomotor and emotion-related behavioral deficits. Few behavior tests of cognitive function have been applied in the s-ICH model. MacLellan et al. (MacLellan et al., 2009) used a series of behavioral tests, including spontaneous alternation, elevated plus maze, open-field, Morris water maze, T-maze, and the radial arm maze test to evaluate learning and memory deficits in a rat s-ICH model, but found no significant differences from control rats. The novel object recognition test was first utilized in the s-ICH model to evaluate recognition memory but yielded no significant results. A clinical study showed a strong relationship between hippocampal volume and cognitive performance (Kliper et al., 2013). In our study, hippocampal volume was unchanged on day 22 post-ICH, which might explain the results.

Post-stroke depression (PSD) affects approximately one-third of patients after stroke (Hacket and Pickles, 2014), but its exact mechanism is not clear. The specific location of a lesion, such as basal ganglia or left frontal lobe, may play an important role in the etiology of PSD (Fang and Cheng, 2009). Prior studies have shown that patients with lesions in the left hemisphere have a high frequency of PSD (Eastwood et al., 1989; Starkstein et al., 1988). However, a recent systematic review of the studies revealed a significant association between right-hemispheric stroke and incidence of depression (Wei et al., 2015). No preclinical studies have investigated depression after right-hemispheric ICH. In our model of right-hemispheric ICH, mice in the s-ICH (10 μl and 30 μl) groups exhibited learned helplessness in the forced swim test and tail suspension test, and anhedonia in the sucrose preference test (Wang et al., 2008b; Zhe et al., 2017). The basal ganglia lesion and atrophy of the ipsilateral cortex and striatum might be the cause of PSD in this s-ICH model. White matter injury negatively affects the prognosis of ICH patients (Zuo et al., 2017). Using MRI and histology, we have detected white matter tract damage in the s-ICH models (Li et al.,

2017b; Yang et al., 2017a; Zhang et al., 2017a). The contribution of white matter injury to PSD and cognitive dysfunction needs further research.

Rats with IVH show locomotor deficiency and spatial memory loss (Ahn et al., 2013; Liu et al., 2017). To our knowledge, no previous studies have evaluated depression-like behaviors after IVH in animals. A recent clinical trial of adult patients with large spontaneous IVH and obstructive hydrocephalus showed a wide range of scores on tests of communication, memory, and emotion, even in subjects with poor outcomes on the modified Rankin score (mRS grades 3–5) (Ziai et al., 2016). Another clinical study showed that patients with aneurysmal subarachnoid hemorrhage had lower scores for verbal memory performance and emotion recognition and more marked depressive symptoms compared to healthy controls (Brand et al., 2015). Our current study revealed that the IVH mice had locomotor deficiency with abnormal recognition memory and depression-like behaviors. Inflammation might be one major mechanisms by which IVH exerts deleterious effects (Hallevi et al., 2012). Elevated proinflammatory cytokines are associated with depression and abnormal cognitive function (Elderkin-Thompson et al., 2012). Our study showed microglia/macrophage activation around the ventricles, which may contribute to depression-like behaviors in this model (Singhal and Baune, 2017). Additionally, the cylinder test with a power of 0.13 did not identify alterations in forelimb use and rotation asymmetry in the IVH model, probably because hematoma can reside in both ventricles and cause bilateral injury. Another unanswered question is whether residual hydrocephalus secondary to IVH may contribute to cognitive or emotional disturbance in the longer term. ICH subjects with IVH extension are at an increased risk for developing incontinence and dysmobility, which often co-exist with cognitive dysfunction (Woo et al., 2016). Furthermore, periventricular white matter tracts are frequently damaged after IVH, mainly due to extracellular hemoglobin toxicity (Ley et al., 2016).

The cortex is the second most common brain region affected by ICH in humans (Xi et al., 2006). Mice with cortical hemorrhage have been reported to display motor dysfunction (Anan et al., 2017; Masuda et al., 2010). In our study, c-ICH mice exhibited locomotor deficiency, abnormal recognition memory, and depression-like behaviors. However, the cylinder test was not sensitive for assessing locomotor asymmetry in the mouse c-ICH model. Similarly, Tennant and Jones (Tennant and Jones, 2009) found the cylinder test to be insensitive for detecting motor deficits in mice with small cortical infarcts. They hypothesized that the small lesion “did not result in sufficient impairments in postural support behaviors with the contralesional forelimb.” Recognition memory was significantly impaired in the c-ICH mice. Neuroinflammation in the hippocampus and prefrontal cortex may induce cognitive deficits (Costa et al., 2014). We showed previously that activated microglia/macrophages, reactive astrocytes, and infiltrating neutrophils accumulate in the perihematomal regions in the c-ICH model at 72 h (Zhu et al., 2014). Enhanced inflammatory response may contribute to the cognitive deficits in the novel object recognition test. In a previous traumatic brain injury model, controlled cortical impact caused brain tissue loss, a decrease in hippocampal volume, and deficits in emotion-related behaviors (Washington et al., 2012). Consistent with that study, we found decreases in volume of the whole brain, ipsilateral cortex, and ipsilateral hippocampus after c-ICH. Furthermore, our data revealed that the depression-like behaviors were not affected by the

lesion size in the cortex. One clinical study showed that infarct located at frontal and temporal lobes was an independent risk factor for early depressive symptoms in the acute stage of stroke (Metoki et al., 2016). This finding indicates that injury to the cortex may result in depression-like behaviors, which can explain why the incidence in the c-ICH group was as high as 50%.

Studies have confirmed that hippocampus is critical for recognition memory (Ahn et al., 2008; Cohen et al., 2013; Danckert et al., 2007). In rats, h-ICH induced by collagenase produced depression-like behaviors that might have been related to the associated apoptosis observed in the hippocampus (Roh et al., 2016). In our study, the h-ICH mice demonstrated abnormal recognition memory and depression-like behaviors. Locomotor function appeared normal except for that in the 24-point neurologic deficit score during the first week. The mild neurologic deficits might have been caused by the compression of the hematoma against the adjacent cortex. It might also be possible that the 24-point neurologic deficit score is more sensitive than the other two locomotor tests. The wire hanging test had a power of only 0.17, which might have been due to small sample size or may suggest that it is not a sensitive behavioral test to evaluate locomotor function after hippocampal injury. Inflammation might contribute to cognitive impairment after stroke. Clinical studies have shown that inflammatory markers are associated with reduced hippocampal volume and poor cognitive performance among stroke survivors (Kliper et al., 2013). In a chronic unpredictable mild stress model in rats, a decrease in hippocampal volume correlated with the impairment of learning and memory (Luo et al., 2014). In our study, microglia/macrophage activation around the hematoma and a decrease in hippocampal volume may contribute to the pathogenesis of these behavioral deficits.

Microglial and macrophage activation and polarization have been well characterized in the perihematomal region in the s-ICH model (Chang et al., 2017; Lan et al., 2017a; Lan et al., 2017b; Zhang et al., 2017b), but not in the IVH, c-ICH, and h-ICH models. Microglial phenotype and function may vary between brain regions, and these differences may explain the variations in brain damage and repair we observed in the four ICH models. In future studies, we will characterize the dynamic changes in microglial phenotype and the longitudinal changes in the inflammatory response in ICH models that affect different brain regions and identify the underlying molecular targets.

In summary, we have established and validated right-hemispheric IVH, c-ICH, and h-ICH models in mice and compared them with the commonly used s-ICH model. We demonstrated that brain damage and behavioral deficits differ by brain region affected. In terms of future preclinical studies, we found that the 24-point neurologic deficit scoring system and wire-hanging test are sensitive for evaluating motor function in all four ICH models; the tail suspension test, forced swim test, and sucrose preference test can be effectively used to evaluate depression-like behavior in all four ICH models; and the novel object recognition test can be used to evaluate recognition memory in the IVH, c-ICH, and h-ICH models.

Supplementary Material

Refer to Web version on PubMed Central for supplementary material.

Acknowledgments

We thank Wei-zhu Tang for help with brain slicing and Mike Musteric and Stephanie Chew for help with blind analysis of histology, immunofluorescence, and behavioral tests. We thank Claire Levine, MS, ELS, for assistance with manuscript preparation; and we thank Raymond Koehler, PhD, and the Wang lab team members for insightful input. This research was supported by the National Natural Science Foundation of China (U1704166), the National Institutes of Health (R01NS078026, R01AT007317, R56NS096549, R21NS101614, and R01NS102583), the American Heart Association (Grant-in-Aid, 17GRNT33660766), and a Stimulating and Advancing ACCM Research (StAAR) grant from the Department of Anesthesiology and Critical Care Medicine, Johns Hopkins University.

Abbreviation

c-ICH	cortical intracerebral hemorrhage
h-ICH	hippocampal intracerebral hemorrhage
ICH	intracerebral hemorrhage
IVH	intraventricular hemorrhage
PSD	post-stroke depression
s-ICH	striatal intracerebral hemorrhage

References

Ahn HJ, Hernandez CM, Levenson JM, Lubin FD, Liou HC, Sweatt JD. c-Rel, an NF-kappaB family transcription factor, is required for hippocampal long-term synaptic plasticity and memory formation. Learn Mem. 2008; 15:539–549. [PubMed: 18626097]

Ahn SY, Chang YS, Sung DK, Sung SI, Yoo HS, Lee JH, Oh WI, Park WS. Mesenchymal stem cells prevent hydrocephalus after severe intraventricular hemorrhage. Stroke. 2013; 44:497–504. [PubMed: 23287782]

Anan J, Hijioka M, Kurauchi Y, Hisatsune A, Seki T, Katsuki H. Cortical hemorrhage-associated neurological deficits and tissue damage in mice are ameliorated by therapeutic treatment with nicotine. J Neurosci Res. 2017; 95:1838–1849. [PubMed: 28066914]

Auriat AM, Colbourne F. Delayed rehabilitation lessens brain injury and improves recovery after intracerebral hemorrhage in rats. Brain Res. 2009; 1251:262–268. [PubMed: 19059222]

Beray-Berthat V, Delifer C, Besson VC, Girgis H, Coqueran B, Plotkine M, Marchand-Leroux C, Margaill I. Long-term histological and behavioural characterisation of a collagenase-induced model of intracerebral haemorrhage in rats. J Neurosci Methods. 2010; 191:180–190. [PubMed: 20600312]

Besheer J, Bevins RA. Impact of nicotine withdrawal on novelty reward and related behaviors. Behav Neurosci. 2003; 117:327–340. [PubMed: 12708529]

Brainin M, Tuomilehto J, Heiss WD, Bornstein NM, Bath PM, Teuschl Y, Richard E, Guekht A, Quinn T. Post Stroke Cognition Study G. Post-stroke cognitive decline: an update and perspectives for clinical research. Eur J Neurol. 2015; 22:229–238. e213–226. [PubMed: 25492161]

Brand C, Alber B, Fladung AK, Knauer K, Konig R, Oechsner A, Schneider IL, Tumani H, Widder B, Wirtz CR, Woischneck D, Kapapa T. Cognitive performance following spontaneous subarachnoid haemorrhage versus other forms of intracranial haemorrhage. Br J Neurosurg. 2014; 28:68–80. [PubMed: 23879444]

Brand S, Zimmerer S, Kalak N, Planta SV, Schwenzer-Zimmerer K, Muller AA, Zeilhofer HF, Holsboer-Trachsler E. Compared to controls, patients with ruptured aneurysm and surgical intervention show increase in symptoms of depression and lower cognitive performance, but their objective sleep is not affected. World J Biol Psychiatry. 2015; 16:96–105. [PubMed: 24564532]

Can A, Dao DT, Arad M, Terrillion CE, Piantadosi SC, Gould TD. The mouse forced swim test. J Vis Exp. 2012a; 59:e3638.

Can A, Dao DT, Terrillion CE, Piantadosi SC, Bhat S, Gould TD. The tail suspension test. J Vis Exp. 2012b:e3769. [PubMed: 22315011]

Chang CF, Wan J, Li Q, Renfroe SC, Heller NM, Wang J. Alternative activation-skewed microglia/macrophages promote hematoma resolution in experimental intracerebral hemorrhage. Neurobiol Dis. 2017; 103:54–69. [PubMed: 28365213]

Cheng T, Wang W, Li Q, Han X, Xing J, Qi C, Lan X, Wan J, Potts A, Guan F, Wang J. Cerebroprotection of flavanol (−)-epicatechin after traumatic brain injury via Nrf2-dependent and -independent pathways. Free Radic Biol Med. 2016; 92:15–28. [PubMed: 26724590]

Christensen MC, Mayer SA, Ferran JM, Kissela B. Depressed mood after intracerebral hemorrhage: the FAST trial. Cerebrovasc Dis. 2009; 27:353–360. [PubMed: 19218801]

Cohen SJ, Munchow AH, Rios LM, Zhang G, Asgeirsdottir HN, Stackman JRW. The rodent hippocampus is essential for nonspatial object memory. Curr Biol. 2013; 23:1685–1690. [PubMed: 23954431]

Costa G, Simola N, Morelli M. MDMA administration during adolescence exacerbates MPTP-induced cognitive impairment and neuroinflammation in the hippocampus and prefrontal cortex. Psychopharmacology (Berl). 2014; 231:4007–4018. [PubMed: 24687411]

Danckert SL, Gati JS, Menon RS, Köhler S. Perirhinal and hippocampal contributions to visual recognition memory can be distinguished from those of occipito-temporal structures based on conscious awareness of prior occurrence. Hippocampus. 2007; 17:1081–1092. [PubMed: 17696171]

De Bundel D, Gangarossa G, Biever A, Bonnefont X, Valjent E. Cognitive dysfunction, elevated anxiety, and reduced cocaine response in circadian clock-deficient cryptochrome knockout mice. Front Behav Neurosci. 2013; 7:152. [PubMed: 24187535]

Eastwood MR, Rifat SL, Nobbs H. Mood disorders following cerebrovascular accident. Br J Psychiatry. 1989; 154:195–200. [PubMed: 2528388]

Elderkin-Thompson V, Irwin MR, Hellemann G, Kumar A. Interleukin-6 and memory functions of encoding and recall in healthy and depressed elderly adults. American Journal of Geriatric Psychiatry. 2012; 20:753–763. [PubMed: 22892560]

Fang J, Cheng Q. Etiological mechanisms of post-stroke depression: a review. Neurol Res. 2009; 31:904–909. [PubMed: 19891854]

Faul F, Erdfelder E, Lang AG, Buchner A. G*Power 3: a flexible statistical power analysis program for the social, behavioral, and biomedical sciences. Behav Res Methods. 2007; 39:175–191. [PubMed: 17695343]

Hacket ML, Pickles K. Part I: frequency of depression after stroke: an updated systematic review and meta-analysis of observational studies. Int J Stroke. 2014; 9:1017–1025. [PubMed: 25117911]

Hallevi H, Albright KC, Aronowski J, Barreto AD, Martin-Schild S, Khaja AM, Gonzales NR, Illoh K, Noser EA, Grotta JC. Intraventricular hemorrhage: Anatomic relationships and clinical implications. Neurology. 2008; 70:848–852. [PubMed: 18332342]

Hallevi H, Walker KC, Kasam M, Bornstein N, Grotta JC, Savitz SI. Inflammatory response to intraventricular hemorrhage: Time course, magnitude and effect of t-PA. Journal of the Neurological Sciences. 2012; 315:93–95. [PubMed: 22126859]

Han X, Lan X, Li Q, Gao Y, Zhu W, Cheng T, Maruyama T, Wang J. Inhibition of prostaglandin E2 receptor EP3 mitigates thrombin-induced brain injury. J Cereb Blood Flow Metab. 2016; 36:1059–1074. [PubMed: 26661165]

Hartman R, Lekic T, Rojas H, Tang J, Zhang JH. Assessing functional outcomes following intracerebral hemorrhage in rats. Brain Res. 2009; 1280:148–157. [PubMed: 19464275]

Hinson HE, Hanley DF, Ziai WC. Management of intraventricular hemorrhage. Curr Neurol Neurosci Rep. 2010; 10:73–82. [PubMed: 20425231]

Hwang BY, Bruce SS, Appelboom G, Piazza MA, Carpenter AM, Gigante PR, Kellner CP, Ducruet AF, Kellner MA, Deb-Sen R, Vaughan KA, Meyers PM, Connolly ES Jr. Evaluation of intraventricular hemorrhage assessment methods for predicting outcome following intracerebral hemorrhage. J Neurosurg. 2012; 116:185–192. [PubMed: 21999319]

Jacobs LF, Gaulin SJ, Sherry DF, Hoffman GE. Evolution of spatial cognition: sex-specific patterns of spatial behavior predict hippocampal size. Proc Natl Acad Sci U S A. 1990; 87:6349–6352. [PubMed: 2201026]

Jiang C, Zuo F, Wang Y, Wan J, Yang Z, Lu H, Chen W, Zang W, Yang Q, Wang J. Progesterone exerts neuroprotective effects and improves long-term neurologic outcome after intracerebral hemorrhage in middle-aged mice. Neurobiol Aging. 2016; 42:13–24. [PubMed: 27143417]

Keep RF, Hua Y, Xi G. Intracerebral haemorrhage: mechanisms of injury and therapeutic targets. The Lancet Neurology. 2012; 11:720–731. [PubMed: 22698888]

Kliper E, Bashat DB, Bornstein NM, Shenhar-Tsarfaty S, Hallevi H, Auriel E, Shopin L, Bloch S, Berliner S, Giladi N, Goldbourt U, Shapira I, Korczyn AD, Assayag EB. Cognitive decline after stroke: relation to inflammatory biomarkers and hippocampal volume. Stroke. 2013; 44:1433–1435. [PubMed: 23444307]

Koivunen RJ, Harno H, Tatlisumak T, Putaala J. Depression, anxiety, and cognitive functioning after intracerebral hemorrhage. Acta Neurol Scand. 2015; 132:179–184. [PubMed: 25639837]

Krafft PR, Rolland WB, Duris K, Lekic T, Campbell A, Tang J, Zhang JH. Modeling intracerebral hemorrhage in mice: injection of autologous blood or bacterial collagenase. J Vis Exp. 2012:e4289. [PubMed: 23023153]

Lan X, Han X, Li Q, Li Q, Gao Y, Cheng T, Wan J, Zhu W, Wang J. Pinocembrin protects hemorrhagic brain primarily by inhibiting toll-like receptor 4 and reducing M1 phenotype microglia. Brain Behav Immun. 2017a; 61:326–339. [PubMed: 28007523]

Lan X, Han X, Li Q, Yang QW, Wang J. Modulators of microglial activation and polarization after intracerebral haemorrhage. Nat Rev Neurol. 2017b; 13:420–433. [PubMed: 28524175]

Langhorne P, Coupar F, Pollock A. Motor recovery after stroke: a systematic review. Lancet Neurol. 2009; 8:741–754. [PubMed: 19608100]

Lee JY, Insel P, Mackin RS, Schuff N, Chui H, DeCarli C, Park KH, Mueller SG, Weiner MW. Different associations of white matter lesions with depression and cognition. BMC Neurol. 2012; 12:83. [PubMed: 22920586]

Ley D, Romantsik O, Vallius S, Sveinsdottir K, Sveinsdottir S, Agyemang AA, Baumgarten M, Morgelin M, Lutay N, Bruschettini M, Holmqvist B, Gram M. High presence of extracellular hemoglobin in the periventricular white matter following preterm intraventricular hemorrhage. Front Physiol. 2016; 7:330. [PubMed: 27536248]

Li Q, Han X, Lan X, Gao Y, Wan J, Durham F, Cheng T, Yang J, Wang Z, Jiang C, Ying M, Koehler RC, Stockwell BR, Wang J. Inhibition of neuronal ferroptosis protects hemorrhagic brain. JCI Insight. 2017a; 2:e90777. [PubMed: 28405617]

Li Q, Wan J, Lan X, Han X, Wang Z, Wang J. Neuroprotection of brain-permeable iron chelator VK-28 against intracerebral hemorrhage in mice. J Cereb Blood Flow Metab. 2017b; 37:3110–3123. [PubMed: 28534662]

Liu DZ, Waldau B, Ander BP, Zhan X, Stamova B, Jickling GC, Lyeth BG, Sharp FR. Inhibition of Src family kinases improves cognitive function after intraventricular hemorrhage or intraventricular thrombin. J Cereb Blood Flow Metab. 2017; 37:2359–2367. [PubMed: 27624844]

Luo Y, Cao Z, Wang D, Wu L, Li Y, Sun W, Zhu Y. Dynamic study of the hippocampal volume by structural MRI in a rat model of depression. Neurol Sci. 2014; 35:1777–1783. [PubMed: 24929958]

MacLellan CL, Auriat AM, McGie SC, Yan RH, Huynh HD, De Butte MF, Colbourne F. Gauging recovery after hemorrhagic stroke in rats: implications for cytoprotection studies. J Cereb Blood Flow Metab. 2006; 26:1031–1042. [PubMed: 16395282]

MacLellan CL, Langdon KD, Churchill KP, Granter-Button S, Corbett D. Assessing cognitive function after intracerebral hemorrhage in rats. Behav Brain Res. 2009; 198:321–328. [PubMed: 19041895]

MacLellan CL, Plummer N, Silasi G, Auriat AM, Colbourne F. Rehabilitation promotes recovery after whole blood-induced intracerebral hemorrhage in rats. Neurorehabil Neural Repair. 2011; 25:477–483. [PubMed: 21343528]

Manaenko A, Fathali N, Williams S, Lekic T, Zhang JH, Tang J. Geldanamycin reduced brain injury in mouse model of intracerebral hemorrhage. Acta Neurochir Suppl. 2011; 111:161–165. [PubMed: 21725749]

Manaenko A, Lekic T, Sozen T, Tsuchiyama R, Zhang JH, Tang J. Effect of gap junction inhibition on intracerebral hemorrhage-induced brain injury in mice. Neurol Res. 2009; 31:173–178. [PubMed: 19298758]

Masuda T, Maki M, Hara K, Yasuhara T, Matsukawa N, Yu S, Bae EC, Tajiri N, Chheda SH, Solomita MA, Weinbren N, Kaneko Y, Kirov SA, Hess DC, Hida H, Borlongan CV. Peri-hemorrhagic degeneration accompanies stereotaxic collagenase-mediated cortical hemorrhage in mouse. Brain Res. 2010; 1355:228–239. [PubMed: 20691669]

Metoki N, Sugawara N, Hagii J, Saito S, Shiroto H, Tomita T, Yasujima M, Okumura K, Yasui-Furukori N. Relationship between the lesion location of acute ischemic stroke and early depressive symptoms in Japanese patients. Ann Gen Psychiatry. 2016; 15:12. [PubMed: 27042194]

Moulin S, Cordonnier C. Prognosis and outcome of intracerebral haemorrhage. Front Neurol Neurosci. 2015; 37:182–192. [PubMed: 26587771]

Moulin S, Labreuche J, Bombois S, Rossi C, Boulouis G, Henon H, Duhamel A, Leys D, Cordonnier C. Dementia risk after spontaneous intracerebral haemorrhage: a prospective cohort study. Lancet Neurol. 2016; 15:820–829. [PubMed: 27133238]

Perez-Urrutia N, Mendoza C, Alvarez-Ricartes N, Oliveros-Matus P, Echeverria F, Grizzell JA, Barreto GE, Iarkov A, Echeverria V. Intranasal cotinine improves memory, and reduces depressive-like behavior, and GFAP+ cells loss induced by restraint stress in mice. Exp Neurol. 2017; 295:211–221. [PubMed: 28625590]

Renard CE, Dailly E, Nic Dhonnchadha BA, Hascoet M, Bourin M. Is dopamine a limiting factor of the antidepressant-like effect in the mouse forced swimming test? Prog Neuropsychopharmacol Biol Psychiatry. 2004; 28:1255–1259. [PubMed: 15588751]

Rogove AD, Lu W, Tsirka SE. Microglial activation and recruitment, but not proliferation, suffice to mediate neurodegeneration. Cell Death Differ. 2002; 9:801–806. [PubMed: 12107823]

Roh JH, Ko IG, Kim SE, Lee JM, Ji ES, Kim JH, Chang HK, Lee SK, Kim KH. Treadmill exercise ameliorates intracerebral hemorrhage-induced depression in rats. J Exerc Rehabil. 2016; 12:299–307. [PubMed: 27656626]

Rubin RD, Watson PD, Duff MC, Cohen NJ. The role of the hippocampus in flexible cognition and social behavior. Front Hum Neurosci. 2014; 8:742. [PubMed: 25324753]

Rynkowski MA, Kim GH, Komotar RJ, Otten ML, Ducruet AF, Zacharia BE, Kellner CP, Hahn DK, Merkow MB, Garrett MC, Starke RM, Cho BM, Sosunov SA, Connolly ES. A mouse model of intracerebral hemorrhage using autologous blood infusion. Nat Protoc. 2008; 3:122–128. [PubMed: 18193028]

Sherry DF, Forbest MRL, Khurgel O, Ivy GO. Females have a larger hippocampus than males in the brood-parasitic brown-headed cowbird. Proc Natl Acad Sci U S A. 1993; 90:7839–7843. [PubMed: 8356091]

Singhal G, Baune BT. Microglia: an interface between the loss of neuroplasticity and depression. Front Cell Neurosci. 2017; 11:270. [PubMed: 28943841]

Starkstein JE, Robinson RG, Berthier ML. Differential mood changes following basal ganglia vs thalamic lesions. Arch Neurol. 1988; 45:725–730. [PubMed: 3390026]

Tang WK, Chen YK, Lu JY, Chu WC, Mok VC, Ungvari GS, Wong KS. Cerebral microbleeds and depression in lacunar stroke. Stroke. 2011; 42:2443–2446. [PubMed: 21757672]

Tennant KA, Jones TA. Sensorimotor behavioral effects of endothelin-1 induced small cortical infarcts in C57BL/6 mice. J Neurosci Methods. 2009; 181:18–26. [PubMed: 19383512]

Vahid-Ansari F, Lagace DC, Albert PR. Persistent post-stroke depression in mice following unilateral medial prefrontal cortical stroke. Transl Psychiatry. 2016; 6:e863. [PubMed: 27483381]

Wang J. Preclinical and clinical research on inflammation after intracerebral hemorrhage. Prog Neurobiol. 2010; 92:463–477. [PubMed: 20713126]

Wang J, Dore S. Inflammation after intracerebral hemorrhage. J Cereb Blood Flow Metab. 2007; 27:894–908. [PubMed: 17033693]

Wang J, Fields J, Dore S. The development of an improved preclinical mouse model of intracerebral hemorrhage using double infusion of autologous whole blood. Brain Res. 2008a; 1222:214–221. [PubMed: 18586227]

Wang J, Rogove AD, Tsirka AE, Tsirka SE. Protective role of tuftsin fragment 1–3 in an animal model of intracerebral hemorrhage. Ann Neurol. 2003; 54:655–664. [PubMed: 14595655]

Wang S, Zhang Z, Guo Y, Zhou H, Teng G, Chen B. Anhedonia and activity deficits in rats: impact of post-stroke depression. Journal of Psychopharmacology. 2008b; 23:295–304. [PubMed: 18562439]

Washington PM, Forcelli PA, Wilkins T, Zapple DN, Parsadanian M, Burns MP. The effect of injury severity on behavior: a phenotypic study of cognitive and emotional deficits after mild, moderate, and severe controlled cortical impact injury in mice. Journal of Neurotrauma. 2012; 29:2283–2296. [PubMed: 22642287]

Wei C, Zhang F, Chen L, Ma X, Zhang N, Hao J. Factors associated with post-stroke depression and fatigue: lesion location and coping styles. J Neurol. 2016; 263:269–276. [PubMed: 26568559]

Wei N, Yong W, Li X, Zhou Y, Deng M, Zhu H, Jin H. Post-stroke depression and lesion location: a systematic review. J Neurol. 2015; 262:81–90. [PubMed: 25308633]

Wells JE, Biernaskie J, Szymanska A, Larsen PH, Yong VW, Corbett D. Matrix metalloproteinase (MMP)-12 expression has a negative impact on sensorimotor function following intracerebral haemorrhage in mice. Eur J Neurosci. 2005; 21:187–196. [PubMed: 15654856]

Woo D, Kruger AJ, Sekar P, Haverbusch M, Osborne J, Moomaw CJ, Martini S, Hosseini SM, Ferioli S, Worrall BB, Elkind MS, Sung G, James ML, Testai FD, Langefeld CD, Broderick JP, Koch S, Flaherty ML. Incontinence and gait disturbance after intraventricular extension of intracerebral hemorrhage. Neurology. 2016; 86:905–911. [PubMed: 26850978]

Wu H, Wu T, Han X, Wan J, Jiang C, Chen W, Lu H, Yang Q, Wang J. Cerebroprotection by the neuronal PGE2 receptor EP2 after intracerebral hemorrhage in middle-aged mice. J Cereb Blood Flow Metab. 2017; 37:39–51. [PubMed: 26746866]

Wu H, Wu T, Xu X, Wang J, Wang J. Iron toxicity in mice with collagenase-induced intracerebral hemorrhage. Journal of Cerebral Blood Flow & Metabolism. 2010; 31:1243–1250. [PubMed: 21102602]

Xi G, Keep RF, Hoff JT. Mechanisms of brain injury after intracerebral haemorrhage. Lancet Neurol. 2006; 5:53–63. [PubMed: 16361023]

Yang J, Li Q, Wang Z, Qi C, Han X, Lan X, Wan J, Wang W, Zhao X, Hou Z, Gao C, Carhuapoma JR, Mori S, Zhang J, Wang J. Multimodality MRI assessment of grey and white matter injury and blood-brain barrier disruption after intracerebral haemorrhage in mice. Sci Rep. 2017a; 7:40358. [PubMed: 28084426]

Yang K, Broussard JI, Levine AT, Jenson D, Arenkiel BR, Dani JA. Dopamine receptor activity participates in hippocampal synaptic plasticity associated with novel object recognition. Eur J Neurosci. 2017b; 45:138–146. [PubMed: 27646422]

Zhang Z, Song Y, Zhang Z, Li D, Zhu H, Liang R, Gu Y, Pang Y, Qi J, Wu H, Wang J. Distinct role of heme oxygenase-1 in early- and late-stage intracerebral hemorrhage in 12-month-old mice. J Cereb Blood Flow Metab. 2017a; 37:25–38. [PubMed: 27317654]

Zhang Z, Zhang Z, Lu H, Yang Q, Wu H, Wang J. Microglial polarization and inflammatory mediators after intracerebral hemorrhage. Mol Neurobiol. 2017b; 54:1874–1886. [PubMed: 26894396]

Zhe Q, Sulei W, Weiwei T, Hongyan L, Jianwei W. Effects of Jiaotaiwan on depressive-like behavior in mice after lipopolysaccharide administration. Metab Brain Dis. 2017; 32:415–426. [PubMed: 27796565]

Zhu W, Cao FS, Feng J, Chen HW, Wan JR, Lu Q, Wang J. NLRP3 inflammasome activation contributes to long-term behavioral alterations in mice injected with lipopolysaccharide. Neuroscience. 2017; 343:77–84. [PubMed: 27923741]

Zhu W, Gao Y, Chang CF, Wan JR, Zhu SS, Wang J. Mouse models of intracerebral hemorrhage in ventricle, cortex, and hippocampus by injections of autologous blood or collagenase. PLoS One. 2014; 9:e97423. [PubMed: 24831292]

Ziai, W., Awad, I., Gregson, B., Mendelow, A., Lees, K., Dawson, J. Clot lysis: Evaluating accelerated resolution of intraventricular hemorrhage (CLEAR III) 365-day results. Presented at European Stroke Organization Conference; Barcelona. 2016.

Zuo S, Pan P, Li Q, Chen Y, Feng H. White matter injury and recovery after hypertensive intracerebral hemorrhage. Biomed Res Int. 2017; 2017:6138424. [PubMed: 28680884]

Highlights

- We evaluated outcomes of ICH that affect right-hemispheric structures in mice.
- ICH was induced in ventricle, cortex, hippocampus, and striatum.
- Motor, cognitive, and emotion-related behaviors were evaluated.
- Brain damage and behavioral deficits after ICH differed by brain region affected.
- This study will help to inform future preclinical studies of ICH outcomes.

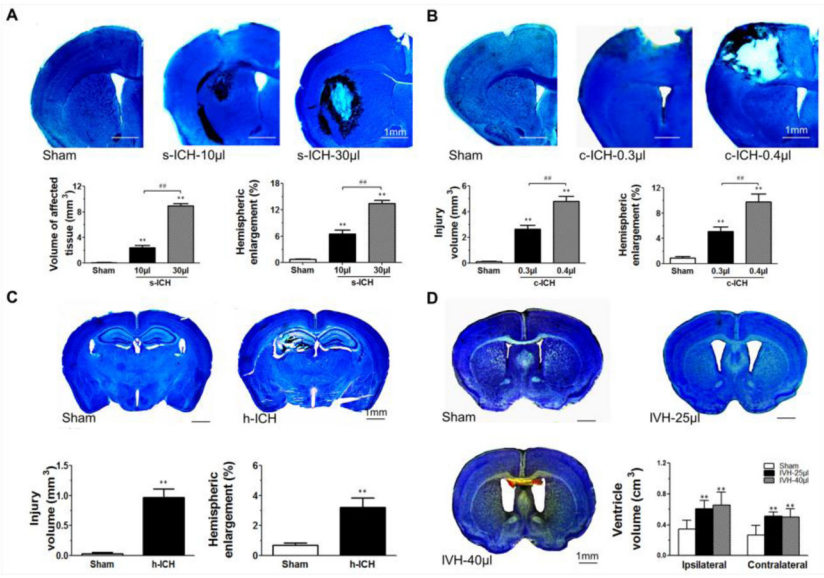

Fig. 1.

Brain injuries in the s-ICH, IVH, c-ICH, and h-ICH mice at 72 h post-ICH. Mouse brains were collected 72 h after ICH or sham procedure, sectioned, and stained with Luxol fast blue/Cresyl (s-ICH, c-ICH, and h-ICH) or Cresyl violet alone (IVH). **(A)** Representative brain sections show hematoma in the right striatum of s-ICH mice injected with 10 μl or 30 μl of autologous blood. Quantification revealed significantly larger volume of affected tissue and hemispheric enlargement in the s-ICH (10 μl and 30 μl) groups than in the sham group. Additionally the volume of affected tissue and degree of hemispheric enlargement were greater in the 30-μl s-ICH group than in the 10-μl s-ICH group (n=6 mice/group, $^{**}P < 0.01$ vs. Sham group, $^{\#\#}P < 0.01$ vs. 10-μl s-ICH group). **(B)** Representative brain sections from sham mice and mice with c-ICH produced by injection of 0.3 or 0.4 μl collagenase. Hematoma was restricted to the right frontal cortex in both low- and high-dose c-ICH groups. Quantification showed significantly larger injury volume and hemispheric enlargement in both c-ICH groups than in the sham group (n=6 mice/group, $^{**}P < 0.01$ vs. Sham group, $^{\#\#}P < 0.01$ vs. low-dose c-ICH group). **(C)** Representative brain sections obtained after sham procedure or h-ICH. Hematoma was present in the right hippocampus in the h-ICH group. Quantification showed significantly larger injury volume and hemispheric enlargement in the h-ICH group than in the sham group (n=6 mice/group, $^{**}P < 0.01$ vs. Sham group). **(D)** IVH was produced by injecting 25 μl or 40 μl of autologous blood into the right ventricle. Quantification showed that both ipsilateral and contralateral ventricular volumes were greater in the IVH mice (25 μl and 40 μl) than in the sham mice (n=6 mice/group, $^{**}P < 0.01$ vs. Sham group), but the difference between the 40-μl IVH group and 25-μl IVH group was not statistically significant ($P > 0.05$). Scale bar = 1 mm. All data are presented as mean ± SD.

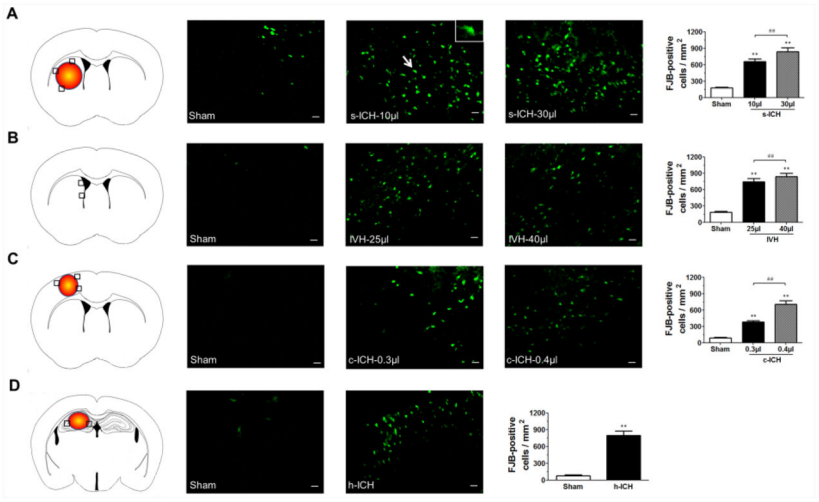

Fig. 2.

Neuronal degeneration in mice at 72 h post-ICH. **(A–D)** The number of FJB-positive cells was elevated in the brain regions around the striatum in s-ICH mice (10 μl and 30 μl, **A**), lateral ventricles in IVH mice (25 μl and 40 μl, **B**), cortex in c-ICH mice (low-dose and high-dose collagenase, **C**), and hippocampus in h-ICH mice (**D**). The black boxes in the schematic diagrams indicate the preselected regions of striatum, lateral ventricles, cortex and hippocampus used for counting FJB-positive cells. Quantification analysis confirmed that significantly more FJB-positive cells were present in the brains of mice that underwent the ICH models than in those of sham mice. Additionally, significantly more FJB-positive cells were present in the brains of mice in the 30-μl s-ICH, 40-μl IVH, and high-dose c-ICH groups than in those of the 10-μl s-ICH, 25-μl IVH, and low-dose c-ICH groups, respectively. Scale bar = 20 μm. All data are presented as mean ± SD; n=6 mice/group; $^{**}P < 0.01$ vs. Sham group; $^{\#\#}P < 0.01$ vs. 10-μl s-ICH group, 25-μl IVH group, or low-dose c-ICH group.

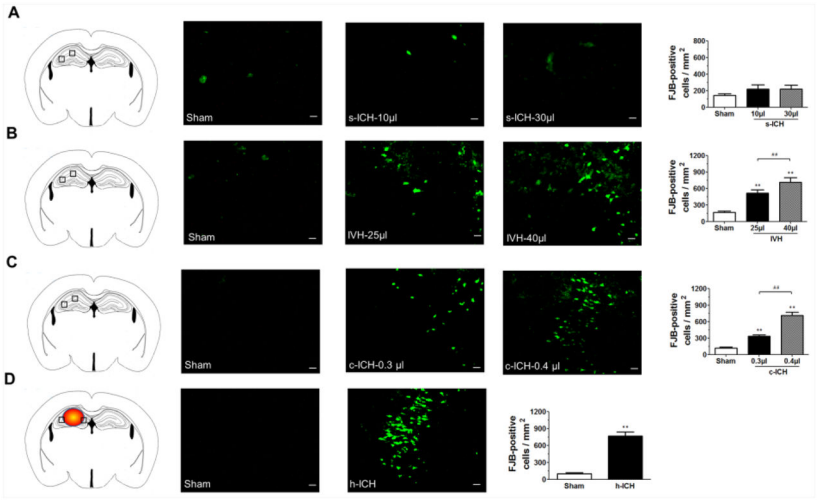

Fig. 3.

Neuronal degeneration in the hippocampus at 72 h post-ICH. **(A–D)** The black boxes in the schematic diagrams indicate the preselected regions of hippocampus used for counting FJB-positive cells. **(A)** The number of FJB-positive cells in the hippocampus was similar in sham and s-ICH mice (both 10-μl and 30-μl groups). However, we observed elevations in the numbers of hippocampal FJB-positive cells in the IVH groups (25 μl and 40 μl, **B**) c-ICH groups (low and high dose, **C**), and h-ICH group (**D**). Quantification analysis showed that significantly more FJB-positive cells were present in the hippocampus of the IVH, c-ICH, and h-ICH groups than in that of the respective sham groups. Additionally, significantly more FJB-positive cells were present in the hippocampus of mice in the 40-μl IVH and high-dose c-ICH groups than in that of the 25-μl IVH and low-dose c-ICH groups, respectively. Scale bar = 20 μm. All data are presented as mean ± SD; n=6 mice/group; $^{**}P < 0.01$ vs. Sham group; $^{\#\#}P < 0.01$ vs. 25-μl IVH group or low-dose c-ICH group.

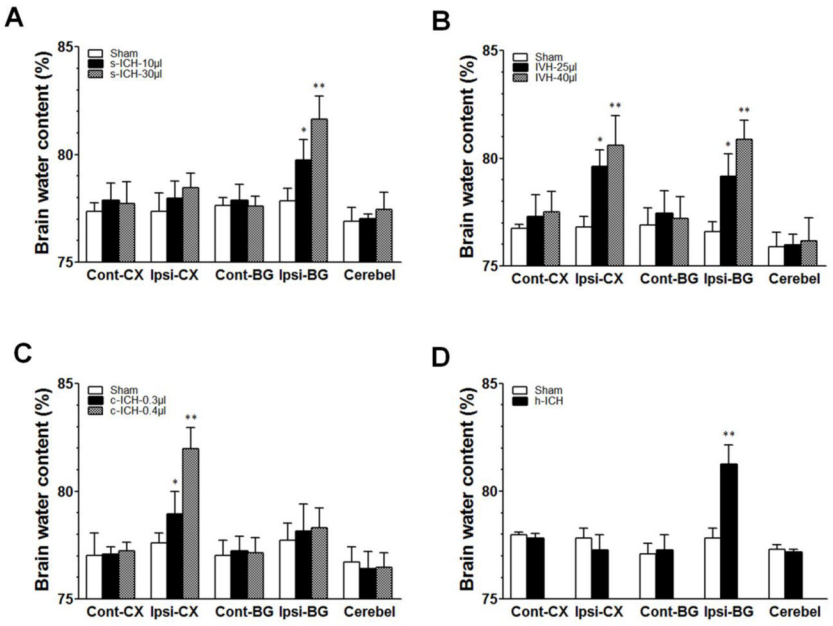

Fig. 4.

Brain edema at 72 h post-ICH. **(A)** Brain water content was increased in the ipsilateral basal ganglia in the s-ICH groups (10 μl and 30 μl) compared with that in the sham group (n=5 mice/group). **(B)** Brain water content was increased in the ipsilateral basal ganglia and cortex of the IVH groups (25 μl and 40 μl) compared with that in the sham group (n=5 mice/group). **(C)** Brain water content was increased in the ipsilateral cortex of the c-ICH groups (low- and high-dose collagenase groups) compared with that in the sham group (n=5 mice/group). **(D)** Brain water content was increased in the ipsilateral basal ganglia of the h-ICH group compared with that in the sham group (n=4 mice/group). All data are presented as mean ± SD; $*P < 0.05$, $**P < 0.01$ vs. Sham group. BG, basal ganglia; Cerebel, cerebellum; Cont, contralateral; CT, cortex; Ipsi, ipsilateral.

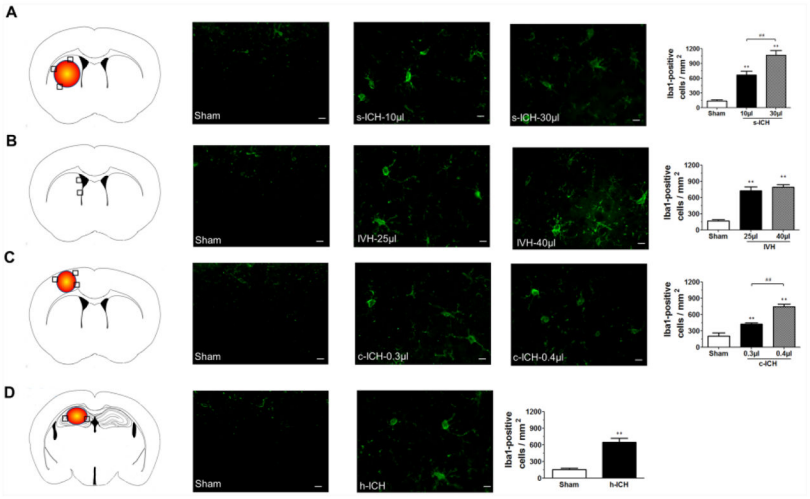

Fig. 5.

Microglia/macrophage activation at 72 h post-ICH. **(A–D)** The black boxes in the schematic diagrams indicate the preselected regions of striatum, lateral ventricles, cortex, and hippocampus used for counting Iba1-positive cells. Compared with that in sham groups, we observed more Iba1-positive activated microglia/macrophages around the injury sites in the striatum of the s-ICH mice (10 μl and 30 μl, **A**), in the brain regions around the lateral ventricles in the IVH mice (25 μl and 40 μl, **B**), around cortex of the c-ICH mice (0.3 μl and 0.4 μl collagenase groups, **C**), and around the hippocampus of the h-ICH mice (**D**). Quantification analysis confirmed that the number of Iba1-positive activated microglia/macrophages was significantly higher in mice that underwent the ICH models than in sham mice, and was significantly higher in the brains of mice in the 30-μl s-ICH and high-dose c-ICH groups than those of the 10-μl s-ICH and low-dose c-ICH groups, respectively. Scale bar = 10 μm. All data are presented as mean ± SD; n=6 mice/group; $^{**}P < 0.01$ vs. Sham group; $^{\#\#}P < 0.01$ vs. 10-μl s-ICH group or low-dose c-ICH group.

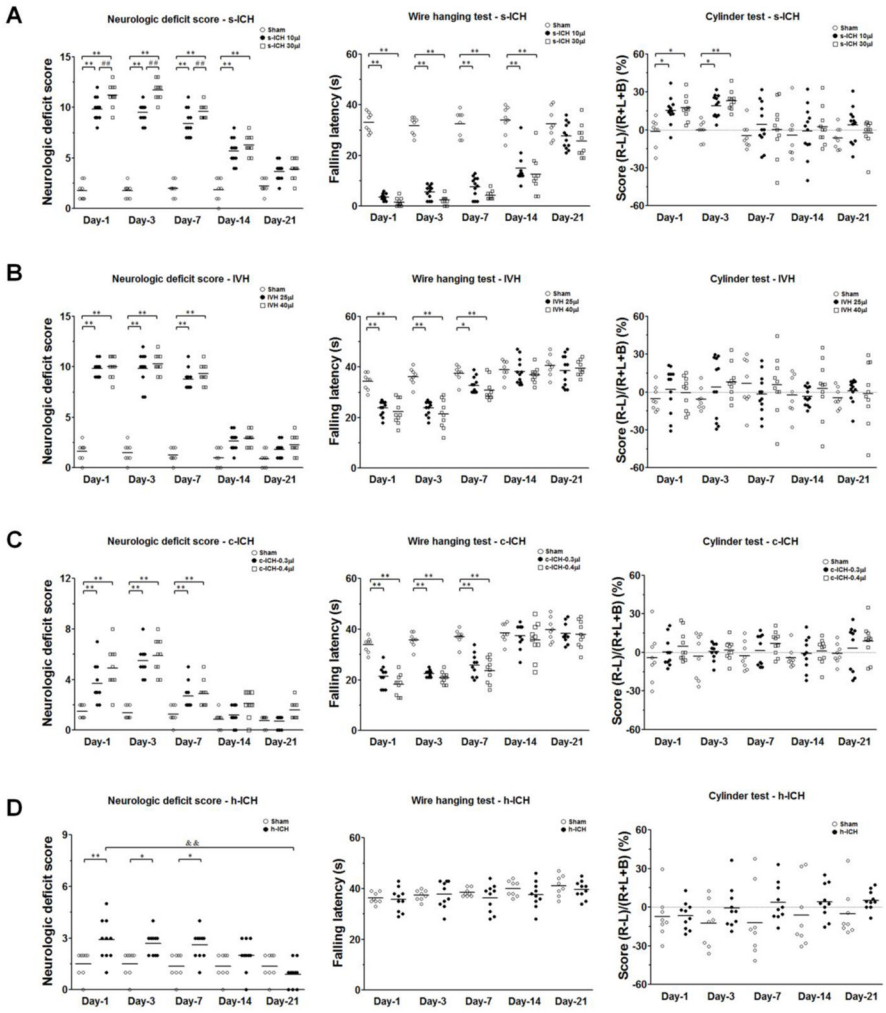

Fig. 6.

Changes in locomotor function after ICH. **(A)** Mice in the s-ICH (10 μl and 30 μl) groups had significantly greater neurologic deficit scores than did mice in the sham group at all time-points. Neurologic deficit scores were significantly higher in the 30-μl s-ICH group than in the 10-μl s-ICH group on days 1, 3, and 7 post-ICH (n=10–12 mice/group). Gripping and forelimb strength were significantly impaired in the s-ICH (10 μl and 30 μl) mice at all time points (n=10–12 mice/group). In the cylinder test, scores were higher in s-ICH (10 μl and 30 μl) mice than in sham mice on days 1 and 3 post-ICH, but no difference was observed between the 30-μl and 10-μl s-ICH mice. The mice exhibited complete recovery on day 7 post-ICH (n=10–12 mice/group). **(B)** Mice in the IVH (25 μl and 40 μl) groups had significantly higher neurologic deficit scores and shorter falling latency in the wire-hanging test than did sham animals on days 1, 3, and 7 post-ICH. However, falling latency in the wire-hanging test did not differ between the 40-μl and the 25-μl IVH mice on those days (n=10–12 mice/group). The mice in each group exhibited no differences in the cylinder test (n=10–12 mice/group, $P > 0.05$). **(C)** Mice in the c-ICH groups exhibited significantly higher neurologic deficit scores than did sham animals on days 1, 3, and 7 post-ICH (n=10 mice/group) as well as marked deficits in gripping and forelimb strength (n=10 mice/group).

The mice did not exhibit differences in the cylinder test (n=10 mice/group, $P > 0.05$); **(D)** Mice in the h-ICH group had significantly higher neurologic deficit scores than did sham animals on days 1, 3, and 7 post-ICH (n=10 mice/group). In the wire-hanging test and the cylinder test, no difference was observed between h-ICH mice and sham animals at any time point (n=10 mice/group, all $P > 0.05$). All data are presented as mean ± SD; $^{*}P < 0.05$, $^{**}P < 0.01$ vs. respective Sham group; $^{\#\#}P < 0.01$ vs. 10-μl s-ICH group; $^{\&\&}P < 0.01$ vs. h-ICH group day 1.

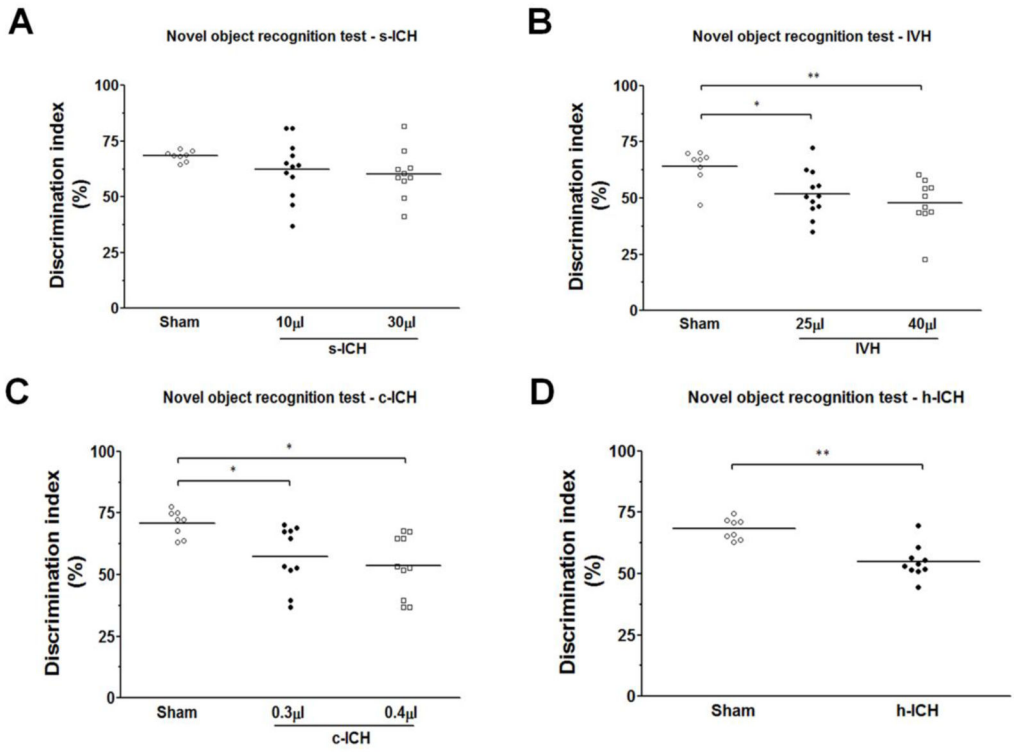

Fig. 7.

Changes in memory function after ICH. Memory was assessed with the novel object recognition test on day 21 in s-ICH, IVH, c-ICH, and h-ICH mice. **(A)** No differences were observed between s-ICH (10 μl and 30 μl) mice and sham animals (n=10–12 mice/group, all $P > 0.05$). **(B)** The discrimination index was significantly smaller in the IVH (25 μl and 40 μl) groups than in the sham group, but no differences were observed between IVH mice injected with 40 μl of blood and those injected with 25 μl of blood (n=10–12 mice/group). **(C, D)** The discrimination index was significantly smaller in the c-ICH (**C**) and h-ICH (**D**) groups than in their respective sham groups (n=10–12 mice/group). All data are presented as mean ± SD; $*P < 0.05$, $**P < 0.01$ vs. Sham group.

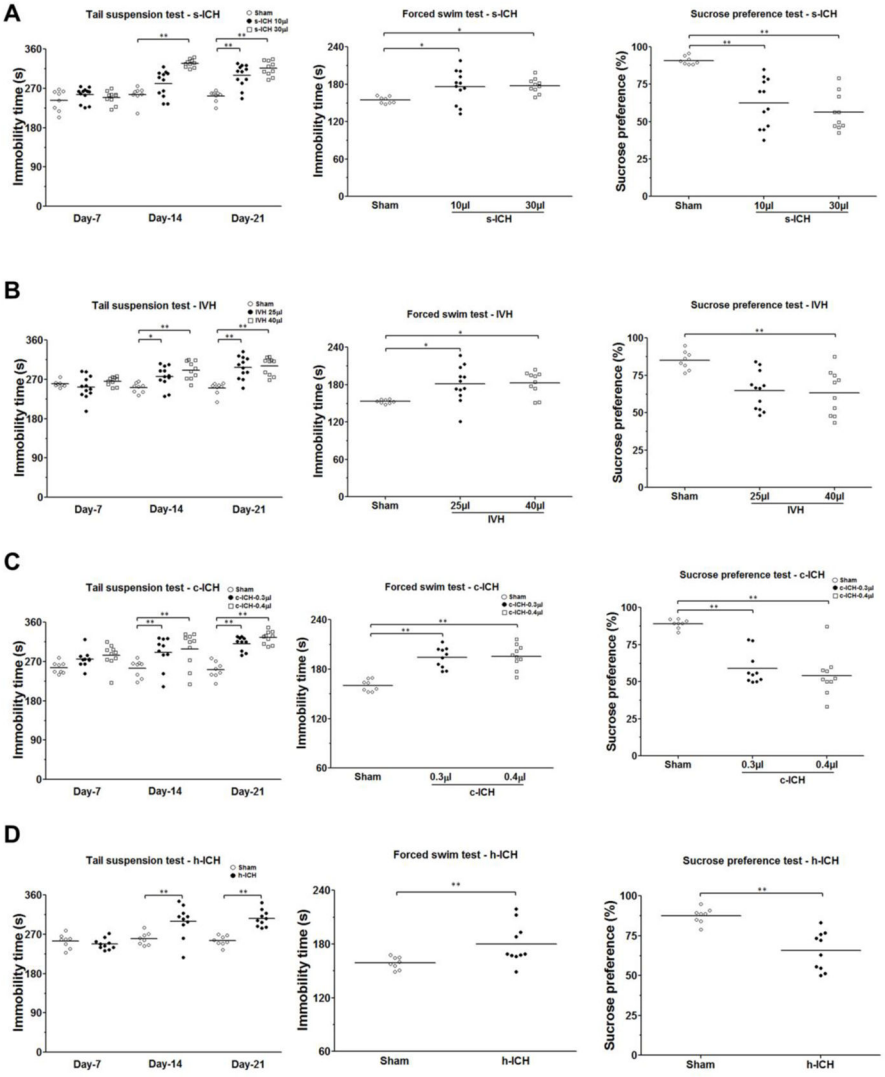

Fig. 8.

Emotional changes after s-ICH, IVH, c-ICH, and h-ICH. **(A)** Mice in the s-ICH (10 μl and 30 μl) groups had significantly longer immobility time than sham animals in the tail suspension test on days 14 and 21 and in the forced swim test on day 22. However, we observed no significant difference between the 10-μl s-ICH group and 30-μl s-ICH group (n=10–12 mice/group). Mice in the s-ICH (10 μl and 30 μl) groups consumed less sucrose than did sham animals in the sucrose preference test (n=10–12 mice/group), but again we observed no difference between the 10-μl s-ICH and 30-μl s-ICH groups. **(B)** Mice in the IVH (25 μl and 40 μl) groups had significantly longer immobility time than sham animals in the tail suspension test on days 14 and 21 and in the forced swim test on day 22. However, no difference was observed between 25-μl IVH and 40-μl IVH groups (n=10–12 mice/group). Only mice in the 40-μl IVH group exhibited a significant decrease in sucrose preference compared to that of sham animals (n=10–12 mice/group). **(C–D)** Mice in the c-ICH **(C)** and h-ICH **(D)** groups had significantly longer immobility times than did sham animals in the tail suspension test on days 14 and 21 and in the forced swim test on day 22.

They also showed less sucrose preference than did sham animals (n=10 mice/group). All data are presented as mean ± SD; *$P < 0.05$, **$P < 0.01$ vs. Sham group.